PROGRESS IN PHOTOVOLTAICS: RESEARCH AND APPLICATIONS
Prog. Photovolt: Res. Appl. 2003; **11**:15–26 (DOI: 10.1002/pip.460)

Research

Analysis of Light Scattering in Amorphous Si:H Solar Cells by a One-Dimensional Semi-coherent Optical Model

Janez Krč*,†, Franc Smole and Marko Topič
Faculty of Electrical Engineering, University of Ljubljana, Tržaška 25, SI-1000 Ljubljana, Slovenia

A one-dimensional semi-coherent optical model for thin-film solar cells is presented. The optical circumstances at flat interfaces are addressed and the situation at rough interfaces in the model is described for the case of direct (coherent) incident and scattered (incoherent) incident light. After the model has been experimentally verified, analysis of the light scattering process in hydrogenated amorphous silicon (a-Si:H) p–i–n solar cells is carried out. The influence of the interface root-mean-square roughness and the effect of different angular distribution functions of diffused light on quantum efficiency and short-circuit current are investigated by the optical model.

KEY WORDS: optical modelling; thin-film solar cells; rough interfaces; light scattering; light trapping; coherent light propagation; incoherent light spreading; scalar scattering theory

I. INTRODUCTION

To enhance light absorption in thin-film solar cells, light trapping is implemented in the multi-layer structures of the solar cells. One of the most commonly used light trapping techniques is scattering of incident light at rough internal interfaces. The roughness of the interfaces is usually achieved by using rough substrates on which the solar cells are deposited. Multi-directional spreading of scattered light in the solar cell increases the optical paths of light propagation in the thin layers, leading to higher absorption. Moreover, higher reflection of scattered light at internal interfaces due to non-perpendicular incidence of the beams at the interfaces assures more efficient light trapping in the solar cells.

The description of light scattering at the rough interfaces of thin-film solar cells presents a comprehensive problem, since the morphology of the interfaces is usually random and their root-mean-square roughness σ_{rms} is of the same order as the wavelength of incident light in the layers. Additionally, the interference pattern which can be observed in the wavelength-dependent characteristics of the solar cells (e.g., quantum efficiency QE) indicates that, besides the scattered light, there still exists a significant amount of direct non-scattered light that propagates coherently throughout the structure.[1]

To analyse and optimise the complex optical process, optical modelling is required. To carry out realistic optical simulations, a model that incorporates both light scattering and coherent propagation of direct light should be used. In order to describe the scattering process in the model: (i) the amount of scattered light at each rough interface; and (ii) how the light is scattered in different directions in reflection and in transmission, have to be determined. Previous publications[2–4] indicate that the amount of scattered light (i) at a rough interface can

* Correspondence to: Janez Krč, Faculty of Electrical Engineering, University of Ljubljana, Tržaška 25, SI-1000 Ljubljana, Slovenia.
† E-mail: Janez.Krc@fe.uni-lj.si

Published online 28 November 2002

Received 4 March 2002
Revised 29 May 2002

be approximately determined by means of scalar scattering theory[5–7] that defines the ratio between diffused (scattered) and total (diffused + specular) light, known as the haze parameter. To describe how the light is scattered in different directions (ii) angular distribution functions of diffused light ADFs, are introduced and determined. Haze and ADFs are scattering parameters that fully characterise scattering process at a rough interface.

Some optical models for thin-film solar cells with rough interfaces have already been reported.[4,8–13] In this paper we present a recently developed one-dimensional semi-coherent optical model. In the model the direct (non-scattered) light is analysed coherently over the entire structure, which is not the case in some of the previously developed optical models.[9,12,13] Thus, the interference pattern in QE of the solar cells can be accurately reproduced in the simulations. For each interface the σ_{rms} value, which determine the haze parameter, and angular distribution functions in reflection and in transmission, can be determined separately. These scattering parameters are input parameters of the model and can be determined (measured) externally for the rough substrate used. Thus, the model can be used for thin-film solar cells deposited on any type of substrate with known (measured) scattering parameters. Describing the light scattering by the scattering parameters involves analysis of enormous amount of data describing the random morphology of rough interfaces in microscopic detail as in some other models.[10] Instead of iterative calculation of direct electromagnetic waves,[4] which are exposed to multiple reflections and transmissions, the distribution of direct light is calculated in one iteration, starting at back and finishing at front side of the structure. All these features enable the simulations to be performed in a few seconds or a few minutes (depending on the structure) without using powerful computers as in case of first principle models, requiring exact description of the interface morphology.[10] In the simulation with the model presented here, not only light scattering at front TCO/*p* and back *n*/metal interfaces is taken into account as in,[9] but scattering at all internal rough interfaces is considered. At a rough interface the interference part of direct light (interaction between forward and backward waves), which may reach 10% of total light intensity,[9] is also considered in the calculation of diffused components at the interface, which neglected is in other reported models. Moreover, additional scattering of already scattered light falling on a rough interface is included and described with different, usually broader angular distribution functions, as in the case of direct incident light. Besides the standard optical quantities (e.g., reflectance R, transmittance T, absorbance A) the model also enables the calculation of carrier generation rate profile in the semiconductor layers which can be incorporated in any standard electrical simulator. In this paper we will restrict our results to absorbance in the layers (enabling calculation of QE and optical losses), total reflectance and short-circuit current, J_{SC}, for the case of a single-junction solar cell structure.

The paper is organised as follows. Optical circumstances at flat interfaces are addressed, and the situation at a rough interface is described for direct incident light in Section II.A and scattered incident light in Section II.B. The simulations carried out using the model are verified with the measured QE of a thin-film hydrogenated amorphous silicon (*a*-Si:H) *p–i–n* solar cell in Section III. The light scattering in the *a*-Si:H *p–i–n* solar cell is analysed. By modelling, the variation of scattering parameters is performed and effects on QE and optical losses investigated. The amount of scattered light (haze parameter) is varied by changing σ_{rms} in simulations and the influence on QE and on J_{sc} are demonstrated in Section IV.A. The role of the *ADF* parameters for direct and scattered incident light is investigated in Section IV.B, C.

II. SEMI-COHERENT OPTICAL MODEL

In an one-dimensional semi-coherent optical model the direct light is treated coherently, in terms of electromagnetic waves, whereas the scattered light is analysed incoherently, owing to its multi-directional spreading. The direct electromagnetic waves are assumed to be harmonic and transversal (TEM).[14] Therefore, it is sufficient to describe them by only one component, i.e., electric field strength E, which is represented by complex number. From the spatial distribution of forward, E^+, and backward waves, E^-, the corresponding light intensities I^+, I^-, K and the total intensity I for a given wavelength λ, and at a given position in the structure x are calculated from Equation (1).

$$\begin{aligned} I(\lambda,x) &= \frac{1}{2}Y_0\left[n(\lambda)\left|E^+(\lambda,x)\right|^2 - n(\lambda)\left|E^-(\lambda,x)\right|^2 - 2k(\lambda)\mathrm{Im}\left[E^-(\lambda,x)E^{+*}(\lambda,x)\right]\right] \\ &= I^+(\lambda,x) - I^-(\lambda,x) - K(\lambda,x) \end{aligned} \tag{1}$$

The intensity K represents the interference contribution (interactions between forward and backward waves), which has either a forward or backward direction, according to the sign of K. In Equation (1) the symbols $n(\lambda)$ and $k(\lambda)$ represent the real and the imaginary part of layer's complex refractive index $N(\lambda) = n(\lambda) - \mathrm{j}k(\lambda)$. Y_0 is the optical admittance of free space ($Y_0 = 2{\cdot}6544 \times 10^{-3}$ S). The asterisk denotes a complex conjugate value, and Im is the imaginary part of the complex number.

Since the scattered light is assumed to be inconherent in the model, its discrete light beams can be represented directly by intensities I^+, I^- and directions (angles) φ of their propagation. At a rough interface, the angular dependence of diffused light is determined by the angular distribution functions ADF_1 in the case of direct incident light, and ADF_2 in the case of scattered incident light. In the model, optical circumstances for direct incident and scattered incident light have to be defined at both flat and rough interfaces over the entire structure. Moreover, owing to multiple reflections at internal interfaces, it has to be considered that the light falls on the interfaces from both left (front) and right (back) directions in general.

At a flat interface, the reflection and transmission of the direct coherent light waves are determined by Fresnel coeficients.[14] By incidence of scattered light at a flat interface each incoherent discrete beam is analysed separately. In this case, the angular-dependent reflectance and transmittance for each incident beam are calculated. The directions of the reflected and transmitted light beams are determined by geometrical optics.[14]

II.A Incidence of direct light at a rough interface

The first situation discussed is the incidence of direct light at a rough interface. A part of direct incident light is scattered into diffused components (dif) in reflection and in transmission, whereas the rest of light does not scatter, and is assigned to the specular components (spec). If the direct incident light is also coherent, the specular component in reflection and in transmission have to preserve the coherence. In the following we analyse the incidence of incoherent light at a rough interface first, since it presents a basis for the analysis of coherent light incidence in our model. If the direct light is incoherent the specular intensity of reflected and transmitted light at rough interfaces in the solar cells can be determined approximately from the equations of scalar scattering theory.[5–7] Assuming illumination from the left-hand side of the interface, the specular reflectance R_{Lspec} and specular transmittance T_{LRspec} are defined by Equations (2 and 3):

$$R_{\mathrm{Lspec}} = R_0 \exp -\left(\frac{4\pi\sigma_{\mathrm{rms}} c_{\mathrm{r}} n_{\mathrm{L}}(\lambda)}{\lambda}\right)^2 \tag{2}$$

$$T_{\mathrm{LRspec}} = T_0 \exp -\left(\frac{4\pi\sigma_{\mathrm{rms}} c_{\mathrm{t}} |n_{\mathrm{L}}(\lambda) - n_{\mathrm{R}}(\lambda)|}{\lambda}\right)^3 \tag{3}$$

The first index of transmittance T indicates the incident medium (left), whereas the second one is the transmitted medium (right). The subscript 'spec' denotes the specular part. R_0 and T_0 are total (spec + dif) reflectance and transmittance, and are assumed to be the same as the reflectance and transmittance at a flat interface. Coefficients c_{r} and c_{t} are correction factors, which can be adjusted for a particular substrate morphology by means of total integrated scattering measurements on the substrates.[15] In our case we assume $c_{\mathrm{r}} = c_{\mathrm{t}} = 1$ in the simulations.[7]

The corresponding diffused reflectance R_{Ldif} and diffused transmittance T_{LRdif} can be easily determined by Equations (4 and 5).

$$R_{\mathrm{Ldif}} = R_0 - R_{\mathrm{Lspec}} \tag{4}$$

$$T_{\mathrm{LRdif}} = T_0 - T_{\mathrm{LRspec}} \tag{5}$$

The haze parameter of a rough interface in reflection and transmission can be defined by $H_{\mathrm{refl}} = \mathrm{R}_{\mathrm{RLdif}}/R_0$ and $H_{\mathrm{trans}} = T_{\mathrm{LRdif}}/T_0$. From Equations (2–5) it can be found out that H_{refl} and H_{trans} depend on σ_{rms}, wavelength and optical constants of the layers forming the interface. On increasing σ_{rms}, haze parameters increase.

For right-side illumination, the indices 'L' and 'R' have to be exchanged consistently in Equations (2–5).

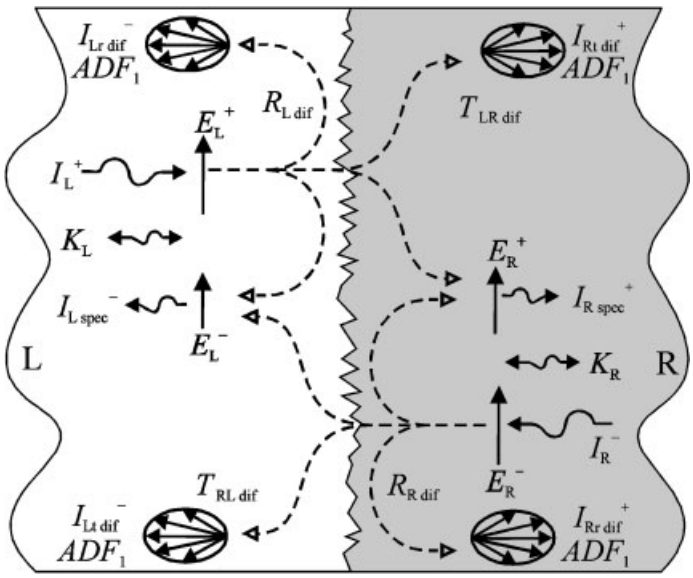

Figure 1. Optical situation at a rough interface on illumination with direct coherent light from both sides of the interface

Since in the model the direct light is treated coherently, Equations (2 and 3) cannot be used directly to calculate the coherent specular intensities. In the following we will briefly describe the approach used in our optical model. A detailed description of the problem is given elsewhere.[16] In Figure 1 a general case of illumination with direct coherent light is applied from both left (L) and right (R) side of the interface. Since in the model the calculation procedure of direct light distribution starts at the right (back) side of the structure at each interface the right-side components, E_R^+ (consisting of reflected and transmitted wave) and E_R^- (incident wave), are known, whereas the specular components at the left side, E_L^+ (incident wave) and E_L^- (reflected and transmitted wave), have to be calculated. First the intensities I_{Rspec}^+, I_{R}^- and K_{R} at the interface are determined by means of Equation (1). Then the interference component K_{R} is added either to I_{Rspec}^+ or I_{R}^-, according to its direction (sign) of propagation. Thus, the interference part is considered in further analysis at a rough interface. With only two resulting light intensities, I_{RK}^+ and I_{RK}^- (not shown in Figure 1), we can calculate the specular light intensities, I_{LK}^+ and I_{LK}^-, incorporating the interference part K_{L} on the left side by Equations (6 and 7). Reflectances and transmittances in Equations (6 and 7) are calculated by means of Equations (2 and 3), as in the case of incoherent light:

$$I_{\mathrm{LK}}^+ = \frac{1}{T_{\mathrm{LRspec}}} I_{\mathrm{RK}}^+ - \frac{R_{\mathrm{Rspec}}}{T_{\mathrm{LRspec}}} I_{\mathrm{RK}}^- \tag{6}$$

$$I_{\mathrm{LK}}^- = \frac{R_{\mathrm{Lspec}}}{T_{\mathrm{LRspec}}} I_{\mathrm{RK}}^+ - \frac{R_{\mathrm{Rspec}} R_{\mathrm{Lspec}} - T_{\mathrm{RLspec}} T_{\mathrm{LRspec}}}{T_{\mathrm{LRspec}}} I_{\mathrm{RK}}^- \tag{7}$$

To establish E_{L}^+ and E_{L}^- from the known I_{LK}^+ and I_{LK}^- we first have to determine the sign of K_{L}. From the general definition of K in Equation (1) (in this case labelled with index L), it can be shown that for the determination of its sign it is sufficient to know only the phases, ϑ_L^+ and ϑ_L^-, of the complex values of the electric field strengths $E_{\mathrm{L}}^+ = |E_{\mathrm{L}}^+| e^{\mathrm{j}\vartheta L+}$ and $E_{\mathrm{L}}^- = |E_{\mathrm{L}}^-| e^{\mathrm{j}\vartheta L-}$. Simulations indicated that these phases have significant influence on the position of the interference pattern in the wavelength-dependent QE of the solar cells. On the basis of similar interference patterns of structures with smooth and moderately rough interfaces we made an assumption that, at a rough interface, one can apply the same phases of electric field strengths as in the case of smooth interfaces. After calculating ϑ_L^+ and ϑ_L^- we can also determine the absolute values $|E_{\mathrm{L}}^+|$ and $|E_{\mathrm{L}}^-|$ from I_{LK}^+ and I_{LK}^- at a rough interface. Thus, the specular parts at the left side are defined. Afterwards, the intensities of the diffused components, I_{Lrdif}^-, I_{Ltdif}^-, I_{Rtdif}^+ and I_{Rrdif}^+ (Figure 1) are calculated from I_{LK}^+ and I_{RK}^- using diffused reflectances R_{Ldif}, R_{Rdif} and diffused transmittances T_{RLdif} and T_{LRdif} (Equations 4 and 5).

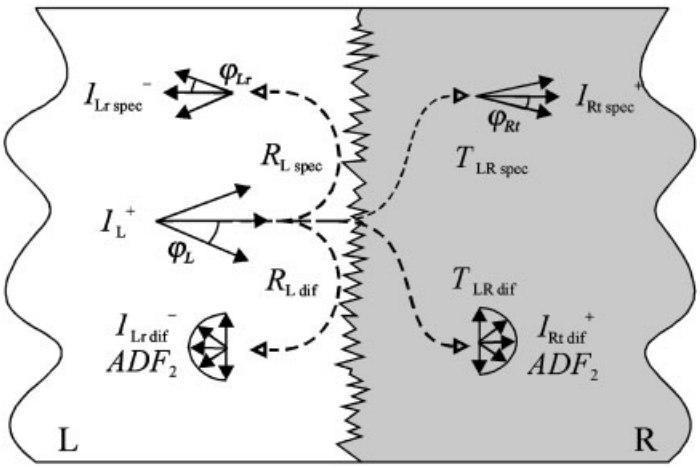

Figure 2. Optical situation at a rough interface on illumination with scattered incoherent light from the left side of the interface

In the case of direct incident light, the angular distribution of the diffused parts in reflection and transmission is described by $\mathrm{ADF}_{1\mathrm{refl}} = \mathrm{ADF}_{1\mathrm{trans}} = \mathrm{ADF}_1$. The ADF_1 is an input parameter of our optical model. For a particular substrate this function can be experimentally determined by means of angular resolved scattering measurements[1] and incorporated in the model. In our case we simulate solar cells deposited on Asahi U-type (glass/SnO_2) substrate. For this type of substrate a normalised $\cos^2$ function was reported to be a fair approximation to the real angular distribution function.[9]

II.B Incidence of scattered light at a rough interface

The second optical situation which has to be defined at a rough interface is the incidence of scattered light. The situation is symbolically illustrated in Figure 2. In this case both scattered incident components I_L^+ and I_R^- are known at the interface in the model. The analysis of left- and right-side illumination can be carried out independently. For this reason, in Figure 2 only the light components referring to left-side illumination are shown. At the interface for each scattered beam the specular reflectance and transmittance are defined. In this case the angular dependency of incident φ_L, reflected, $\varphi_{\mathrm{Lr}} = \varphi_\mathrm{L}$ and transmitted light beams φ_{Rt} have to be taken into account. Following the scalar scattering theory, the angular-dependent R_{Lspec} and T_{LRspec} are defined by Equations (8 and 9).

$$R_{\mathrm{Lspec}}(\varphi_\mathrm{L}, \varphi_{\mathrm{Rt}}) = R_0(\varphi_\mathrm{L}, \varphi_{\mathrm{Rt}})\ \exp - \left(\frac{4\pi\sigma_{\mathrm{rms}} c_\mathrm{r} n_\mathrm{L}(\lambda)\cos\varphi_\mathrm{L}}{\lambda}\right)^2 \tag{8}$$

$$T_{\mathrm{LRspec}}(\varphi_\mathrm{L}, \varphi_{\mathrm{Rt}}) = T_0(\varphi_\mathrm{L}, \varphi_{\mathrm{Rt}}) \exp - \left(\frac{4\pi\sigma_{\mathrm{rms}} c_\mathrm{t} |n_\mathrm{L}(\lambda)\cos\varphi_\mathrm{L} - n_\mathrm{R}(\lambda)\cos\varphi_{\mathrm{Rt}}|}{\lambda}\right)^3 \tag{9}$$

The directions (angles) of reflected and transmitted specular beams φ_{Lr} and φ_{Rt} are calculated by geometric optics, as in the case of a flat interface.

For diffused light an average reflectance $\bar{R}_{\mathrm{Ldif}}$ and transmittance $\bar{T}_{\mathrm{Ldif}}$ are defined by Equations (10 and 11), respectively, where the $\mathrm{ADF}_{\mathrm{inc}}$ represents the angular distribution function of the incident scattered light I_L^+. The $\mathrm{ADF}_{\mathrm{inc}}$ is determined by light beams that approach the interface.

$$\bar{R}_{\mathrm{Ldif}} = \sum_{\varphi_L} \mathrm{ADF}_{\mathrm{inc}}(\varphi_\mathrm{L}) \left[R_0(\varphi_\mathrm{L}, \varphi_{\mathrm{Rt}}) - R_{\mathrm{Lspec}}(\varphi_\mathrm{L}, \varphi_{\mathrm{Rt}})\right] \tag{10}$$

$$\bar{T}_{\mathrm{Ldif}} = \sum_{\varphi_\mathrm{L}} \mathrm{ADF}_{\mathrm{inc}}(\varphi_\mathrm{L}) \left[T_0(\varphi_\mathrm{L}, \varphi_{\mathrm{Rt}}) - T_{\mathrm{LRspec}}(\varphi_\mathrm{L}, \varphi_{\mathrm{Rt}})\right] \tag{11}$$

The angular distribution function of the diffused parts in the case of scattered incident light, ADF_2, has to be broader than ADF_1 since the incident light is already scattered in different directions. In our simulations we approximate the $ADF_{2refl} = ADF_{2trans} = ADF_2$ with half-circular distribution, as indicated in Figure 2.

In the analysis of right-side illumination, the same Equations (8–11) can be used, subject to consistent 'L' and 'R' index exchange. The procedure of calculation in entire multi-layer structures can be found elsewhere.[16]

III. VERIFICATION OF THE MODEL

With our optical model, we carried out the simulation of a single junction *a*-Si:H *p–i–n* solar cell structure, deposited on commercially available Asahi U-type substrate, consisting of glass and rough SnO_2 transparent conductive oxide (TCO) layer. The TCO thickness was 650 nm. Its surface roughness σ_{rms} was measured as 40 nm. The solar cells were made in a superstrate glass/TCO/*p–i–n*/Ag configuration. The thicknesses of the *p*(*a*-SiC:H)–*i*(*a*-Si:H)–*n*(*a*-Si:H) layers are 10–300–20 nm. The surface roughness of the substrate is transferred to all internal interfaces of the thin-film solar cell structure. The same $\sigma_{rms} = 40$ nm of all rough interfaces is assumed in the simulation.

The measured (circles) and simulated (thick full line) QE of a representative solar cell are given in Figure 3. The experimental data of the QE, optical constants of the layers and the value of the σ_{rms} of the TCO surface were provided by the Delft University of Technology.[7] In calculations of the QE, a simplified, but justified, electrical analysis was applied, assuming the ideal extraction of charge carriers from the active *i*-layer and neglecting the contribution of the *p*- and *n*-layers.[7] To include optical losses at real *n*/Ag interface in the analysis, a 1·5-nm-thick buffer layer with optical properties of Al was introduced between the *n*-layer and Ag layer.[17] In the simulation, the normalised $\cos^2\varphi$ function was used for ADF_1 and the half-circular distribution for ADF_2. Also in the figure also the simulated optical losses represented by absorbance, *A*, in TCO, *p*-, *n*- and Ag* (buffer + Ag) layer are shown by thin lines. Additionally, the amount of reflected light from the solar cell is indicated by the $1 - R$ curve.

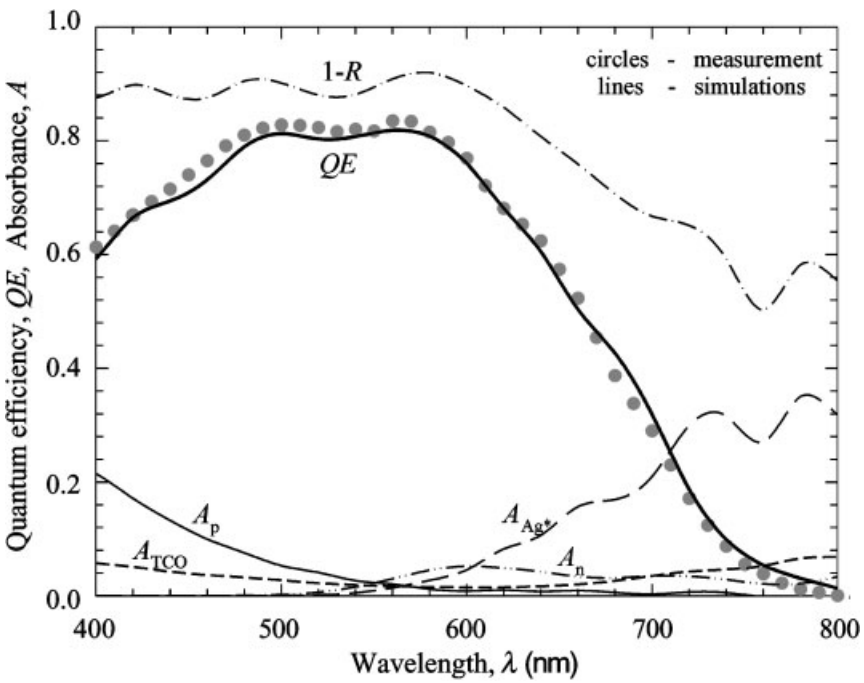

Figure 3. Measured (circles) and simulated (thick full line) quantum efficiency of the *a*-Si:H *p–i–n* solar cell. The calculated absorbances in TCO, *p*-, *n*- and Ag* (buffer + Ag) layers and the $1-R$ curve are included

Table I. Measured and simulated J_{sc} determined from QE for the *a*-Si:H *p–i–n* solar cell under AM1·5 illumination

	σ_{rms} (nm)	ADF_1	ADF_2	J_{sc} (mA/cm^2)*
Measurement	40			14·31
Simulation (a)	10			12·13
	40	$\cos^2$	1:1	14·48
	80			15·77
Simulation (b)		5:1		13·10
	40	1:1	1:1	14·58
		1:5		14·40
Simulation (c)			5:1	13·62
	40	$\cos^2$	1:1	14·48
			1:5	15·34

*Determined from QE.

From the measured and simulated QE, short-circuit current of the solar cell J_{sc}, under AM1·5 illumination was calculated (Table I). The simulated QE in Figure 3 and the calculated J_{sc} are in good agreement with the experimental data. In particular, the position and intensity of the interference pattern of the QE, which cannot be obtained with incoherent optical models, matches well with the measured one. The fringes of the pattern are only moderately pronounced in the short-wavelength region, since the roughness of the solar cell substrate is relatively high.

The advantages of the semi-coherent optical model become more evident if a substrate with a lower roughness is used ($\sigma_{rms} < 40$ nm), as shown in Section IV, or in the case of a structure with a lower number of rough interfaces (e.g., cells with flat substrate and textured back reflector).

The model was also verified on other types of *a*-Si:H structures (e.g., multi-terminal colour detectors[18]). Recently, it has been applied also to different *a*-Si:H solar cell structures (different thicknesses of *i*-layer[19]) and deposited on a different substrate of different roughnesses (glass/ZnO:Al[15]). Good agreement was obtained in all the cases, indicating the validity and credibility of the presented optical model.

IV. ANALYSIS OF LIGHT SCATTERING IN AN *A*-SI:H SOLAR CELL WITH THE OPTICAL MODEL

On the basis of the good agreement between simulated and measured QE and J_{sc} we use the semi-coherent model for further optical investigation. To analyse the effect of light scattering on QE and J_{sc} we change the amount of scattered light by changing σ_{rms} (haze) of the substrate and internal interfaces. Additionally, the influence of angular distribution of scattered light (ADF_1 and ADF_2) is investigated.

IV.A analysis of σ_{rms} variation

A separate analysis of σ_{rms} variation is carried out. In Figure 4 we present the simulated QE of the *a*-Si:H solar cell in the same configuration as previously, only one parameter of the rough interface, σ_{rms}, is varied. Changing the σ_{rms}, the haze parameters of the substrate and of the internal interfaces are varied. The simulations for three different roughnesses, $\sigma_{rms} = 10$ nm (short-dashed line), $\sigma_{rms} = 40$ nm (full line) and $\sigma_{rms} = 80$ nm (long-dashed line) are shown in the figure. Two effects can be observed: (i) increasing σ_{rms} the QE increases at longer wavelengths ($\lambda > 500$ nm); and (ii) the interference pattern becomes less pronounced. Both effects are a consequence of the enhanced amount of scattered light (increased haze) in the structure, and can also be observed experimentally.

Increasing σ_{rms}, the J_{sc} also increases as shown in Table I(a). Simulations indicate that at higher roughnesses ($\sigma_{rms} > 60$ nm) the J_{sc} of the analysed solar cell starts to saturate (not investigated here). For a realistic

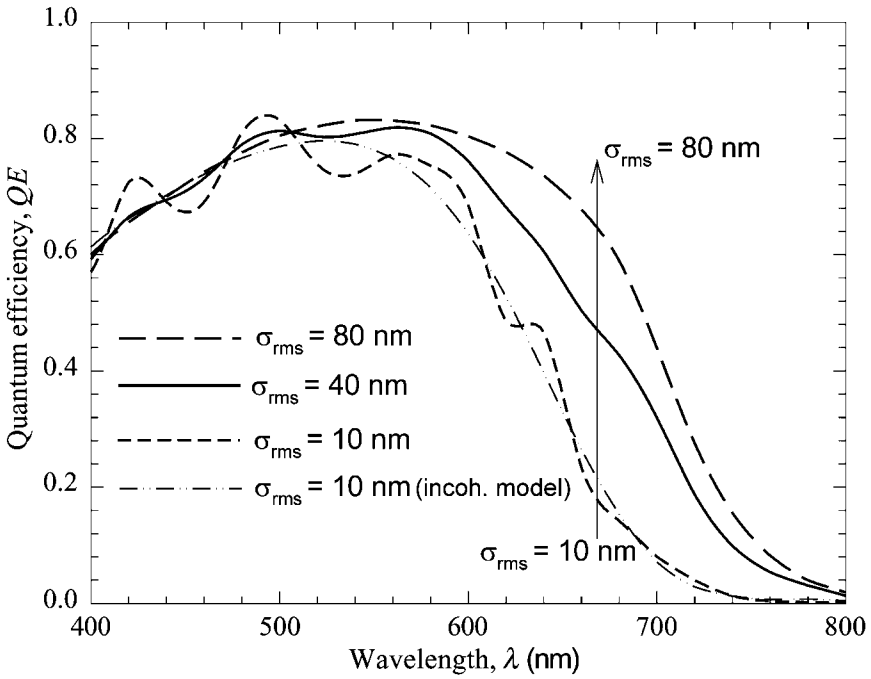

Figure 4. Simulated QE of the *a*-Si:H *p–i–n* solar cell with different σ_{rms} using the semi-coherent model. For $\sigma_{\mathrm{rms}} = 10\,\mathrm{nm}$ one simulated QE based on the incoherent model is given for comparison

investigation of saturation effects it has to be considered that, on changing the σ_{rms} of the substrate, the ADFs may also change, affecting the saturation.

To demonstrate the advantages of the semi-coherent optical model, the simulation of QE obtained with an incoherent optical model[12] for $\sigma_{\mathrm{rms}} = 10\,\mathrm{nm}$ is also given in Figure 4. No interference pattern can be observed, leading to evident deviations between the simulations with the two models. The discrepancy of the incoherent model decreases with increasing σ_{rms}.

IV.B Analysis of ADF$_1$ variation

In Figure 5 we present the results of analysis of ADF_1 variation. In this case we separately investigate the role of angular-dependent scattering properties of the substrate and other rough interfaces on the solar cell performances. The *a*-Si:H solar cell with $\sigma_{\mathrm{rms}} = 40\,\mathrm{nm}$ was used and the ADF_2 was set to a half-circular distribution in all cases. We apply elliptical distributions with different ratios of horizontal to vertical radius (5:1, 1:1 and 1:5) in order to vary ADF_1. The results of simulations are shown in Figure 5 and Table I(b). For comparison the simulation with a normalised $\cos^2$ function is added. Broadening of the ADF_1 (changing the elliptic ratio from 5:1 to 1:5) results in enhanced QE at longer wavelengths ($\lambda > 550\,\mathrm{nm}$) and reduced QE at shorter wavelengths. Simulations show that the decrease in QE at shorter wavelengths is mostly a consequence of increased absorption in the thin *p*-layer, A_{P} (Figure 5), especially, leading to optical losses. The A_{P} is increased by broad-angle scattering at the first interface, TCO/*p*, especially, where the intensity of direct incident light is relatively large, and is pronounced at shorter wavelengths where the absorption coefficients of the *a*-Si:H layers are high. In contrast to the short-wavelength light, most of the long-wavelength light with broader angular distribution function penetrates through the *p*-layer, scatters further at the *p–i* interface and spreads across the active *i*-layer. Multiple reflections and scattering processes at the back and front interfaces of the structure additionally increase the absorption of the broadly scattered long-wavelength light in the *i*-layer, and decrease the reflection, as indicated by $1-R$ curve in Figure 5. Optical losses in the metal contact and in the TCO layer are also

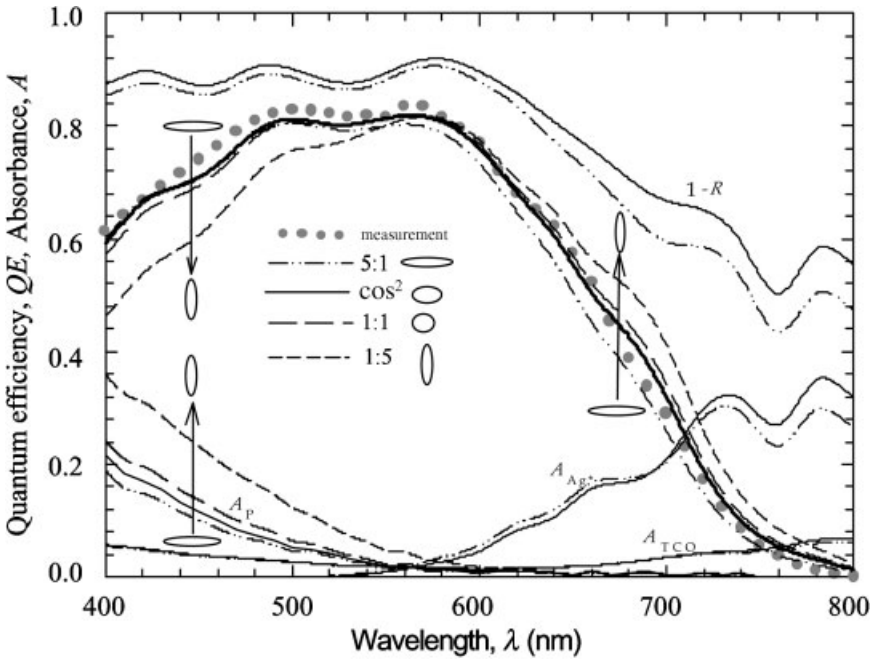

Figure 5. Effects of ADF_1 variation on QE and absorptances in TCO, *p*- and Ag* layer. The reflected light is indicated by 1–*R* curves

enhanced. Among the ADF_1 distributions analysed, the simulation with normalised $\cos^2$ function gives the best agreement with the experimental data, as also indicated by the ADF measurements reported elsewhere.[9]

The increase in J_{sc}, shown in Table I(b), as a consequence of changing the ellipsis ratio from 5:1 to 1:1 can be explained by enhanced QE at longer wavelengths, whereas the decrease in J_{sc} on changing the ratio from 1:1 to 1:5 is a consequence of reduced QE at shorter wavelengths.

IV.C Analysis of ADF_2 variation

The results of ADF_2 variation are presented in Figure 6. By changing the ADF_2 we vary the scattering properties of rough interfaces for the case of scattered incident light and investigate the effects on solar cell performance. Half-elliptical distributions with different ratios of horizontal to vertical radius were applied to the ADF_2. For ADF_1, a normalised $\cos^2$ distribution and, for the interface roughness, $\sigma_{rms} = 40$ nm are used in all the cases. In the figure the simulations of the QE and absorbances in the layers corresponding the elliptic ratios 5:1, 1:1 and 1:5 are plotted. The results show that broadening of ADF_2 (changing the ratio from 5:1 to 1:5) increases the QE, especially at longer wavelengths, and decreases the reflection, as shown in the figure. Optical losses in other layers are slightly increased. Long-wavelength light is not absorbed as efficiently in the *a*-Si:H layers as short-wavelength light, therefore its multi-scattering with broad ADF_2 contributes beneficially to a higher absorption in the active *i*-layer (higher QE). The benefits are also reflected in the J_{sc} values in Table I(c).

V. DISCUSSION

In reality, the parameters σ_{rms}, and angular distribution functions ADF_1 and ADF_2 are coupled and determined by the morphology of a rough interface. To relate haze parameter with the morphology of the rough interfaces the equations of scalar scattering theory can be used. For the substrates with random morphology the relation between angular distribution functions and vertical and lateral parameters of the morphology is still under investigation. Despite not knowing the exact analytical relation between rough interface morphology and its

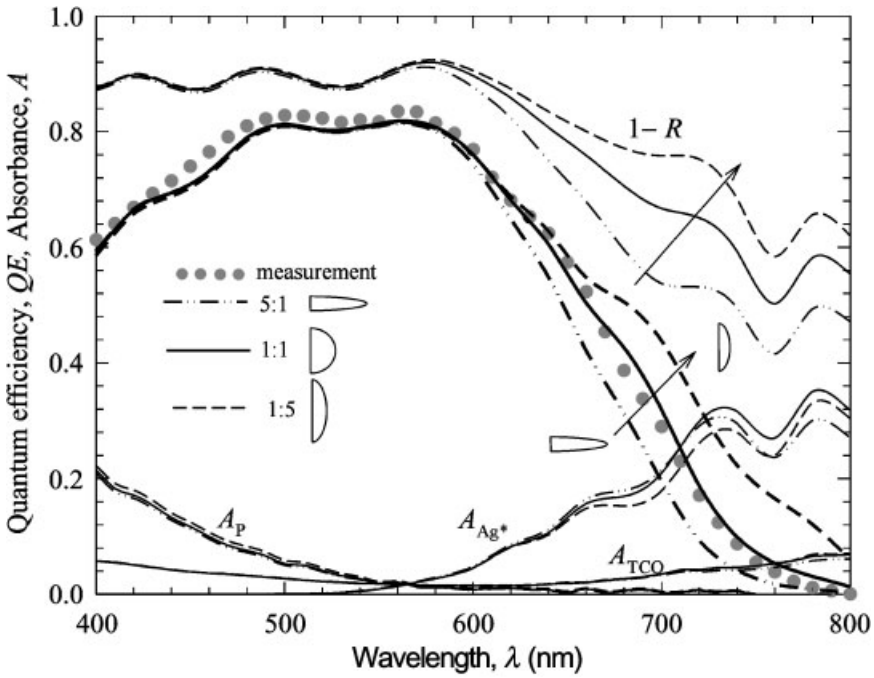

Figure 6. Effects of ADF_2 variation on QE and absorptances in TCO, *p*- and Ag* layer. The reflected light is indicated by 1–*R* curves

scattering parameters it is crucial to know the separate effects of changing the scattering parameters (haze σ_{rms} and angular distribution functions) on the solar cell performances in the search for a substrate with optimal scattering properties. Only optical modelling provides the means to investigate the influence of each parameter separately and to reveal their influence and importance.

The simulation results of the *a*-Si:H solar cell analysed indicate that increasing the σ_{rms} of the interfaces from 10 to 80 nm and keeping the ADF_1 and ADF_2 constant improves the QE and enhances the J_{sc} of the solar cell. Since the increase in σ_{rms} leads to a higher amount of scattered light and consequently to a higher light absorption in the *a*-Si:H *i*-layer, its thickness can be decreased, assuring a better stability of the *a*-Si:H solar cells and lower material costs.[2]

Broadening the ADF_1 of the rough interfaces reveals a trade-off between optical losses for short-wavelength light and the enhancement in QE at longer wavelengths. Accordingly, it has to be pointed out that the substrate with a broad angular distribution function does not necessarily assure better optical performance of solar cells. For a certain substrate with σ_{rms} and a given solar cell configuration the analysis of ADF_1 has to be performed first to predict the possible optical benefits. Further, the presented simulations of ADF_2 variation reveal that the ADF_2 should be as broad as possible since it increases the absorption of long-wavelength light in the *i*-layer, leading to a higher QE and J_{sc} of the solar cell analysed.

All these results show that the haze parameter (determined by σ_{rms}), which is usually used to describe scattering properties of the rough interfaces is not sufficient to judge the scattering characteristics of the substrate and other rough interfaces. The angular distribution functions ADF_1 and ADF_2 are also of importance, as indicated by simulations.

Incorporating the measured scattering parameters, the model can be used for accurate simulations of different solar cell structures deposited on different types of textured substrates. With the model realistic limits in improving light trapping and other optical properties (e.g., optical losses) of solar cells and other types of thin-film structures may be estimated in the future. Further work on the analytical relation between optimised scattering parameters and interface morphology is required to judge between better and worse substrate morphologies.

VI. CONCLUSIONS

For investigation of the light scattering process in *a*-Si:H solar cells a recently developed one-dimensional semi-coherent optical model was utilised. The optical situation at flat interfaces was addressed and optical circumstances at rough interfaces in the model presented. At rough interfaces two angular distribution functions were used to describe the distribution of diffused light at incidence of direct light (ADF_1) and scattered incident light (ADF_2) at a rough interface. The model was verified and used to analyse the influence of scattering parameters, σ_{rms} (haze), ADF_1 and ADF_2, on QE and J_{sc} of the *a*-Si:H solar cell. The increase of σ_{rms} enhances QE and J_{sc}. Broadening of ADF_1 in simulations reveals a trade-off between increased optical losses in the *p*-layer at shorter wavelengths and enhanced absorption of long-wavelength light in the *i*-layer. Broadening of ADF_2 beneficially increases the absorption in the *i*-layer, especially at longer wavelengths. The optical model can be used for the analysis of other types of thin-film solar cells with different scattering properties.

Acknowledgement

The authors are very grateful to M. Zeman of DIMES, Delft University of Technology, for the experimental data and useful discussions.

REFERENCES

1. Stiebig H, Brammer T, Repmann T, Kluth O, Senoussaoui N, Lambertz A, Wagner H. Light scattering in microctystalline silicon thin-film solar cells. *Proceedings of the 16th E-PVSEC*, Glasgow, 2000; 549–552.
2. Schropp REI, Zeman M. *Amorphous and Microcrystalline Silicon Solar Cells: Modeling, Materials and Device Technology.* Kluwer: Norwell, MA, 1998.
3. Brüggemann R, Housé F. Surface roughness and optical scattering in microcrystalline silicon. *Proceedings of the 16th E-PVSEC*, Glasgow, 2000; 641–644.
4. Poruba A, Fejfar A, Remeš Z, Špringer J, Vaneček M, Kočka J. Optical absorption and light scattering in microcrystalline silicon thin films and solar cells. *Journal of Applied Physics* 2000; **88**: 148–160.
5. Bennett HE, Porteus JO. Relation between surface roughness and specular reflectance at normal incidence. *Journal of the Optical Society of America* 1961; **51**: 123–129.
6. Beckmann P, Spizzichino A. *The Scattering of Electromagnetic Waves from Rough Surfaces.* Pergamon, 1963.
7. Zeman M, van Swaaij RACMM, Metselaar JW. Optical modelling of *a*-Si:H solar cells with rough interfaces: effect of back contact and interface roughness. *Journal of Applied Physics* 2000; **88**: 6436–6443.
8. Leblanc F, Perrin J, Schmitt J. Numerical modeling of the optical properties of amorphous silicon based PIN solar cells deposited on rough transparent conducting oxide substrates. *Journal of Applied Physics* 1994; **75**: 1074–1087.
9. Tao G, Zeman M, Metselaar JW. Accurate generation rate profiles in *a*-Si:H solar cells with textured TCO substrates. *Solar Energy Materials and Solar Cells* 1994; **34**: 359–366.
10. Hishikawa Y, Tari H, Kiyama S. Numerical analysis on the optical confinement and optical loss in high-efficiency *a*-Si solar cells with textured surfaces. *Proceedings of the 11th PVSEC*, Sapporo, 1999; 219–220.
11. Sopori B, Madjdpour J, Zhang Y, Chen W, Guha S, Yang J, Banerjee A, Hegedus S. Optical modeling of *a*-Si solar cells. *Materials Research Society Symposium Proceedings* 1999; **557**: 755–760.
12. Krč J, Topič M, Vukadinović M, Smole F. Optical modelling of *a*-Si:H-based solar cells with smooth and rough boundaries. *Proceedings of the 16th E-PVSEC*, Glasgow, 2000; 522–525.
13. Daey Ouwens J, Zeman M, Löffler J, Schropp REI. Sensitivity of optical constants to the spectral absorption in *a*-Si:H solar cells. *Proceedings of the 16th E-PVSEC*, Glasgow, 2000; 405–408.
14. Jin Au Kong. *Electromagnetic Wave Theory.* Wiley: New York, NY, 1990.
15. Krč J, Zeman M, Kluth O, Smole F, Topič M. Experimental investigation and modelling of light scattering in *a*-Si:H solar cells deposited on glass/ZnO:Al substrates. *Materials Research Society Symposium Proceedings* 715, 2002; A13.3.1–A13.3.6.
16. Krč J, Smole F, Topič M. One-dimensional semi-coherent optical model for thin-film solar cells with rough interfaces. *Informacije MIDEM* 2002; **32**(1): 6–13.

17. Stiebig H, Kreisel A, Winz K, Schultz N, Beneking C, Eichoff Th, Wagner H. Spectral response modelling of a-Si:H solar cells. *Proceedings of the 1st World Conference on Photovoltaic Energy Conversion*, Hawaii, 1994; 603–606.
18. Krč J, Topič M, Smole F. Optical modelling of *a*-Si:H-based three-terminal three-colour detectors. *Journal of Non-Crystalline Solids* 2000; **266–269**: 1183–1187.
19. Krč J, Zeman M, Topič M, Smole F, Metselaar JW. Analysis of light scattering in *a*-Si:H-based PIN solar cells with rough interfaces. *Solar Energy Materials and Solar Cells*, 74/1–4, 2002; 401–406.

